October 25, 2021 - GReCO Seminar

Residual eccentricity of binary orbits at the gravitational wave detection threshold: estimates using post-Newtonian theory

Alexandria Tucker

Clifford M. Will

University of Florida

Eccentricity

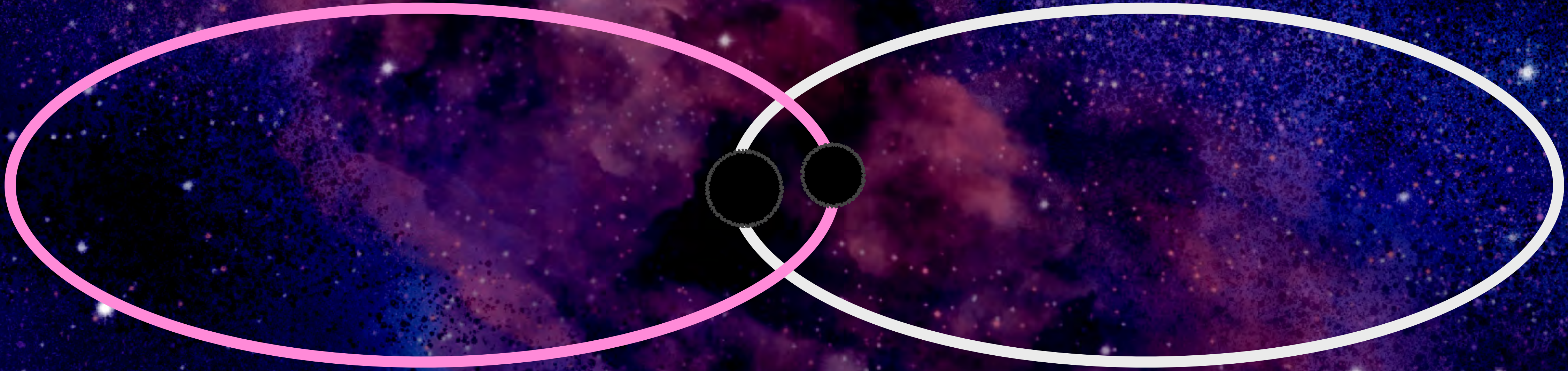

Eccentricity

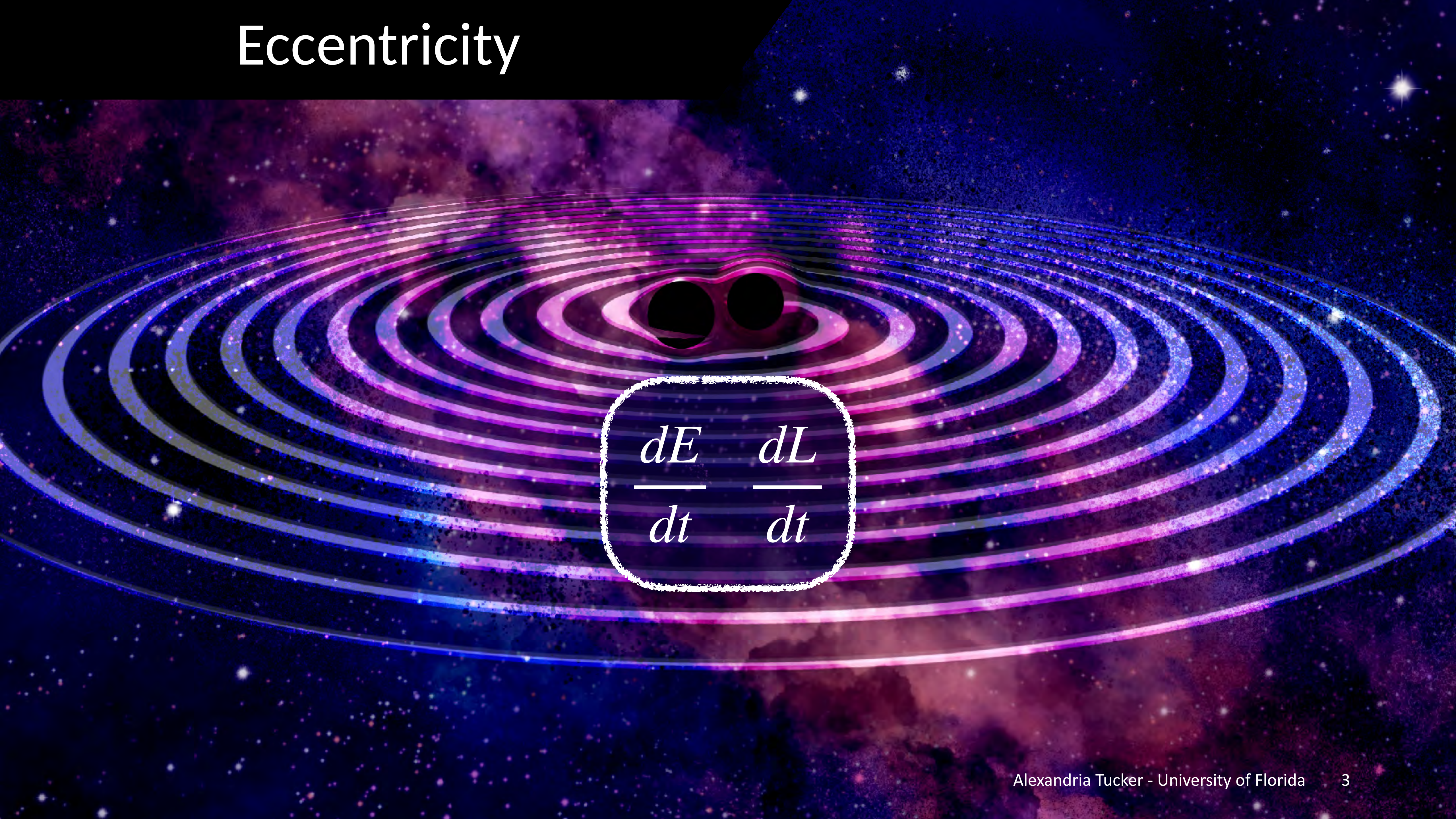

$$\frac{dE}{dt} \qquad \frac{dL}{dt}$$

Eccentricity

Example:

Hulse-Taylor binary pulsar B1913+16

Current eccentricity = 0.617

Crosses LIGO-Virgo threshold in 390 million years

By this time, eccentricity will have decreased to

$$5 \times 10^{-6}$$

Eccentricity

Reasons for residual eccentricities

- not enough time to circularize
- three-body processes
- direct capture

globular clusters | active galactic nuclei

Eccentricity

Implications

The detection and measurement of eccentric inspiral events could serve to **confirm or distinguish among various proposed <u>formation channels</u>**!

Eccentricity

Eccentric binary detection

Current waveform templates used for LIGO-Virgo are **based on quasi-circular models.**

This may **reduce their efficiency** to detect eccentric binaries.

Considerable effort in this direction is ongoing.

preliminary evidence of a highly eccentric merger in GW190521

Our work

Residual eccentricity of inspiralling orbits at the gravitational-wave detection threshold: Accurate estimates using post-Newtonian theory

Alexandria Tucker[1,*] and Clifford M. Will[1,2,†]

Tucker & Will, in Press, *Phys. Rev. D* arXiv:2108.12210

We develop **an accurate map** from the initial parameters of an arbitrarily eccentric binary orbit to the eccentricity when the gravitational wave frequency reaches a detection threshold for a given detector.

Scope and approach

Initial eccentricity ≈ 0.999 Arbitrary mass ratios η Schwarzschild limit (spin = 0)

post-Newtonian theory

Osculating orbit elements

Two-timescale analysis

Tucker & Will, in Press, *Phys. Rev. D* arXiv:2108.12210

post-Newtonian Theory

(Blanchet, Iyer 2003)

$$\vec{a} = -\frac{Gm}{r^2}\hat{n} + \frac{Gm}{r^2}\left(\mathscr{A}_{\mathrm{c}}\,\hat{n} + \frac{1}{\dot{r}}\mathscr{B}_{\mathrm{c}}\,\vec{v}\right) + \frac{8}{5}\eta\frac{Gm}{r^2}\frac{Gm}{rc^3}\left(\dot{r}\mathscr{A}_{\mathrm{rr}}\,\hat{n} + \mathscr{B}_{\mathrm{rr}}\,\vec{v}\right) + \vec{a}_{\mathrm{Tail}}$$

$$\mathcal{A}_{\mathrm{c}}^{(N)} = \sum_{l,m,n} a_{lmn}^{(N)}\frac{\delta_{l+m+n,N}}{c^{2N}}\left(\frac{Gm}{r}\right)^{l}\left(\dot{r}^2\right)^{m}\left(v^2\right)^{n}$$

$$\mathcal{B}_{\mathrm{c}}^{(N)} = \sum_{l,m,n} b_{lmn}^{(N)}\frac{\delta_{l+m+n,N}}{c^{2N}}\left(\frac{Gm}{r}\right)^{l}\left(\dot{r}^2\right)^{m}\left(v^2\right)^{n}$$

$$\mathcal{A}_{\mathrm{rr}}^{(N)} = \sum_{l,m,n} c_{lmn}^{(N)}\frac{\delta_{l+m+n,N}}{c^{2N}}\left(\frac{Gm}{r}\right)^{l}\left(\dot{r}^2\right)^{m}\left(v^2\right)^{n}$$

$$\mathcal{B}_{\mathrm{rr}}^{(N)} = \sum_{l,m,n} d_{lmn}^{(N)}\frac{\delta_{l+m+n,N}}{c^{2N}}\left(\frac{Gm}{r}\right)^{l}\left(\dot{r}^2\right)^{m}\left(v^2\right)^{n}$$

$$\begin{aligned}
\mathcal{A} = {} & \frac{1}{c^2}\left\{-\frac{3\dot{r}^2\nu}{2} + v^2 + 3\nu v^2 - \frac{m}{r}(4+2\nu)\right\} + \frac{1}{c^4}\left\{\frac{15\dot{r}^4\nu}{8} - \frac{45\dot{r}^4\nu^2}{8} - \frac{9\dot{r}^2\nu v^2}{2}\right. \\
& + 6\dot{r}^2\nu^2 v^2 + 3\nu v^4 - 4\nu^2 v^4 + \frac{m}{r}\left(-2\dot{r}^2 - 25\dot{r}^2\nu - 2\dot{r}^2\nu^2 - \frac{13\nu v^2}{2} + 2\nu^2 v^2\right) \\
& \left. + \frac{m^2}{r^2}\left(9 + \frac{87\nu}{4}\right)\right\} + \frac{1}{c^5}\left\{-\frac{24\dot{r}\nu v^2}{5}\frac{m}{r} - \frac{136\dot{r}\nu}{15}\frac{m^2}{r^2}\right\} \\
& + \frac{1}{c^6}\left\{-\frac{35\dot{r}^6\nu}{16} + \frac{175\dot{r}^6\nu^2}{16} - \frac{175\dot{r}^6\nu^3}{16} + \frac{15\dot{r}^4\nu v^2}{2} - \frac{135\dot{r}^4\nu^2 v^2}{4} + \frac{255\dot{r}^4\nu^3 v^2}{8}\right. \\
& - \frac{15\dot{r}^2\nu v^4}{2} + \frac{237\dot{r}^2\nu^2 v^4}{8} - \frac{45\dot{r}^2\nu^3 v^4}{2} + \frac{11\nu v^6}{4} - \frac{49\nu^2 v^6}{4} + 13\nu^3 v^6 \\
& + \frac{m}{r}\left(79\dot{r}^4\nu - \frac{69\dot{r}^4\nu^2}{2} - 30\dot{r}^4\nu^3 - 121\dot{r}^2\nu v^2 + 16\dot{r}^2\nu^2 v^2 + 20\dot{r}^2\nu^3 v^2\right. \\
& \left. + \frac{75\nu v^4}{4} + 8\nu^2 v^4 - 10\nu^3 v^4\right) + \frac{m^2}{r^2}\left(\dot{r}^2 + \frac{32\,573\dot{r}^2\nu}{168} + \frac{11\dot{r}^2\nu^2}{8} - 7\dot{r}^2\nu^3\right. \\
& + \frac{615\dot{r}^2\nu\pi^2}{64} - \frac{26\,987\nu v^2}{840} + \nu^3 v^2 - \frac{123\nu\pi^2 v^2}{64} - 110\dot{r}^2\nu\ln\left(\frac{r}{r_0'}\right) \\
& \left.\left. + 22\nu v^2\ln\left(\frac{r}{r_0'}\right)\right) + \frac{m^3}{r^3}\left(-16 - \frac{41\,911\nu}{420} + \frac{44\lambda\nu}{3} - \frac{71\nu^2}{2} + \frac{41\nu\pi^2}{16}\right)\right\},
\end{aligned}$$

$$\begin{aligned}
\mathcal{B} = {} & \frac{1}{c^2}\{-4\dot{r} + 2\dot{r}\nu\} + \frac{1}{c^4}\left\{\frac{9\dot{r}^3\nu}{2} + 3\dot{r}^3\nu^2 - \frac{15\dot{r}\nu v^2}{2} - 2\dot{r}\nu^2 v^2 + \frac{m}{r}\left(2\dot{r} + \frac{41\dot{r}\nu}{2} + 4\dot{r}\nu^2\right)\right\} \\
& + \frac{1}{c^5}\left\{\frac{8\nu v^2}{5}\frac{m}{r} + \frac{24\nu}{5}\frac{m^2}{r^2}\right\} + \frac{1}{c^6}\left\{-\frac{45\dot{r}^5\nu}{8} + 15\dot{r}^5\nu^2 + \frac{15\dot{r}^5\nu^3}{4} + 12\dot{r}^3\nu v^2\right. \\
& - \frac{111\dot{r}^3\nu^2 v^2}{4} - 12\dot{r}^3\nu^3 v^2 - \frac{65\dot{r}\nu v^4}{8} + 19\dot{r}\nu^2 v^4 + 6\dot{r}\nu^3 v^4 \\
& + \frac{m}{r}\left(\frac{329\dot{r}^3\nu}{6} + \frac{59\dot{r}^3\nu^2}{2} + 18\dot{r}^3\nu^3 - 15\dot{r}\nu v^2 - 27\dot{r}\nu^2 v^2 - 10\dot{r}\nu^3 v^2\right) \\
& \left. + \frac{m^2}{r^2}\left(-4\dot{r} - \frac{18\,169\dot{r}\nu}{840} + 25\dot{r}\nu^2 + 8\dot{r}\nu^3 - \frac{123\dot{r}\nu\pi^2}{32} + 44\dot{r}\nu\ln\left(\frac{r}{r_0'}\right)\right)\right\}.
\end{aligned}$$

Tucker & Will, in Press, *Phys. Rev. D* arXiv:2108.12210

post-Newtonian Theory

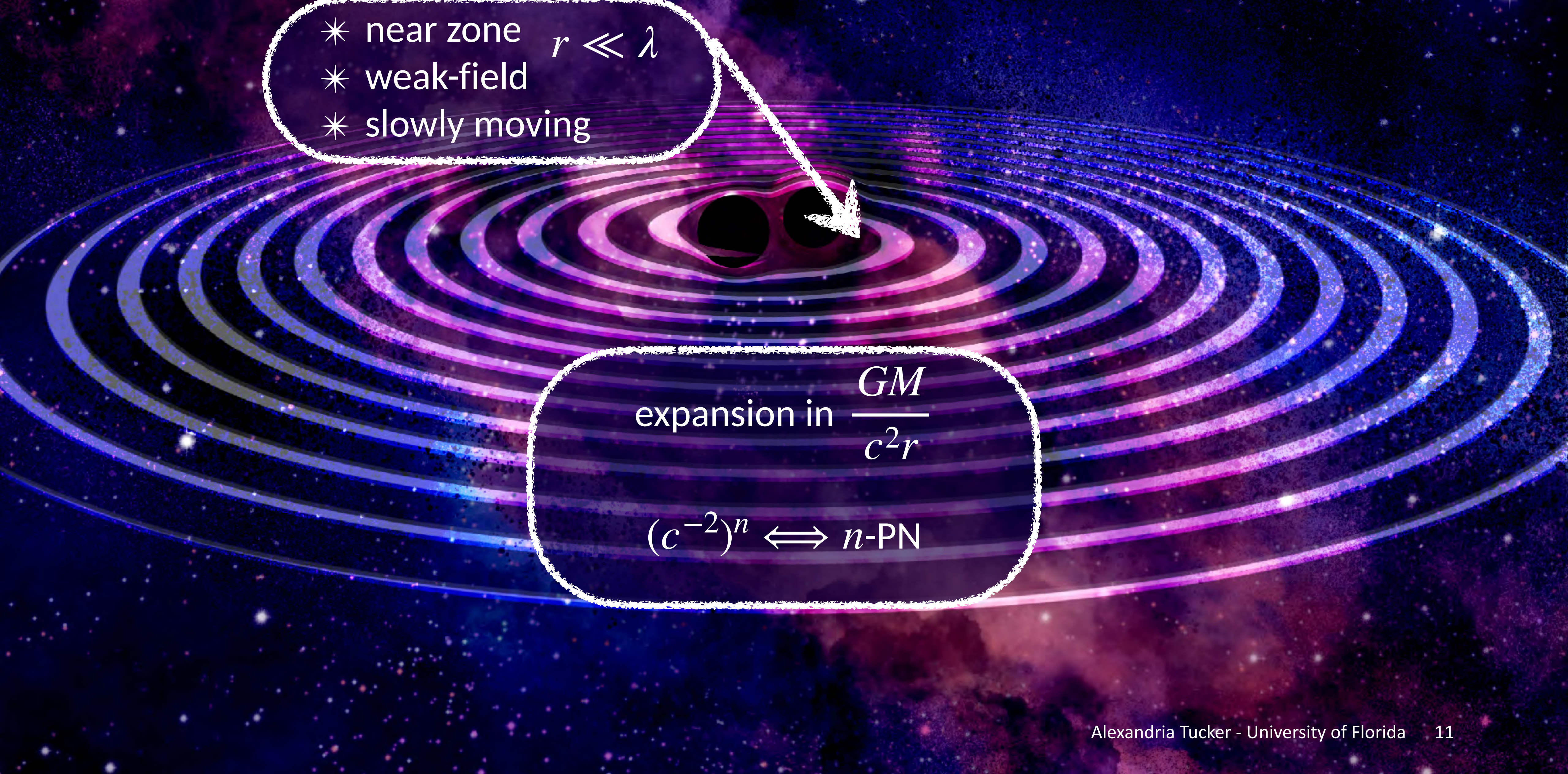

- near zone $r \ll \lambda$
- weak-field
- slowly moving

expansion in $\dfrac{GM}{c^2 r}$

$(c^{-2})^n \iff n\text{-PN}$

Scope and approach

post-Newtonian theory

$$\vec{a} = -\frac{Gm}{r^2}\hat{n} + \frac{Gm}{r^2}\left(\mathscr{A}_{\mathrm{c}}\hat{n} + \frac{1}{\dot{r}}\mathscr{B}_{\mathrm{c}}\vec{v}\right) + \frac{8}{5}\eta\frac{Gm}{r^2}\frac{Gm}{rc^3}\left(\dot{r}\mathscr{A}_{\mathrm{rr}}\hat{n} + \mathscr{B}_{\mathrm{rr}}\vec{v}\right) + \vec{a}_{\mathrm{Tail}}$$

Conservative to 3PN

Radiation reaction (RR)
2.5PN, 3.5PN, & 4.5PN

Lowest order tail - 4PN
(Pati & Will, 2018)

Tucker & Will, in Press, *Phys. Rev. D* arXiv:2108.12210

Scope and approach

Initial eccentricity ≈ 0.999 Arbitrary mass ratios η Schwarzschild limit (spin = 0)

post-Newtonian theory

Osculating orbit elements

Two-timescale analysis

Tucker & Will, in Press, *Phys. Rev. D* arXiv:2108.12210

Osculating orbit elements

Perturbed Kepler Problem

$$\vec{a} = -\frac{Gm}{r^2}\hat{n} + \underbrace{\frac{Gm}{r^2}\left(\mathscr{A}_{\mathrm{c}}\hat{n} + \frac{1}{\dot{r}}\mathscr{B}_{\mathrm{c}}\vec{v}\right) + \frac{8}{5}\eta\frac{Gm}{r^2}\frac{Gm}{rc^3}\left(\dot{r}\mathscr{A}_{\mathrm{rr}}\hat{n} + \mathscr{B}_{\mathrm{rr}}\vec{v}\right) + \vec{a}_{\mathrm{Tail}}}_{\delta\vec{a}}$$

Tucker & Will, in Press, *Phys. Rev. D* arXiv:2108.12210

Osculating orbit elements

radial cross-track out of plane

$$\delta\vec{a} = \mathcal{R}\hat{n} + \mathcal{S}\hat{\lambda} + \mathcal{W}\hat{h}$$

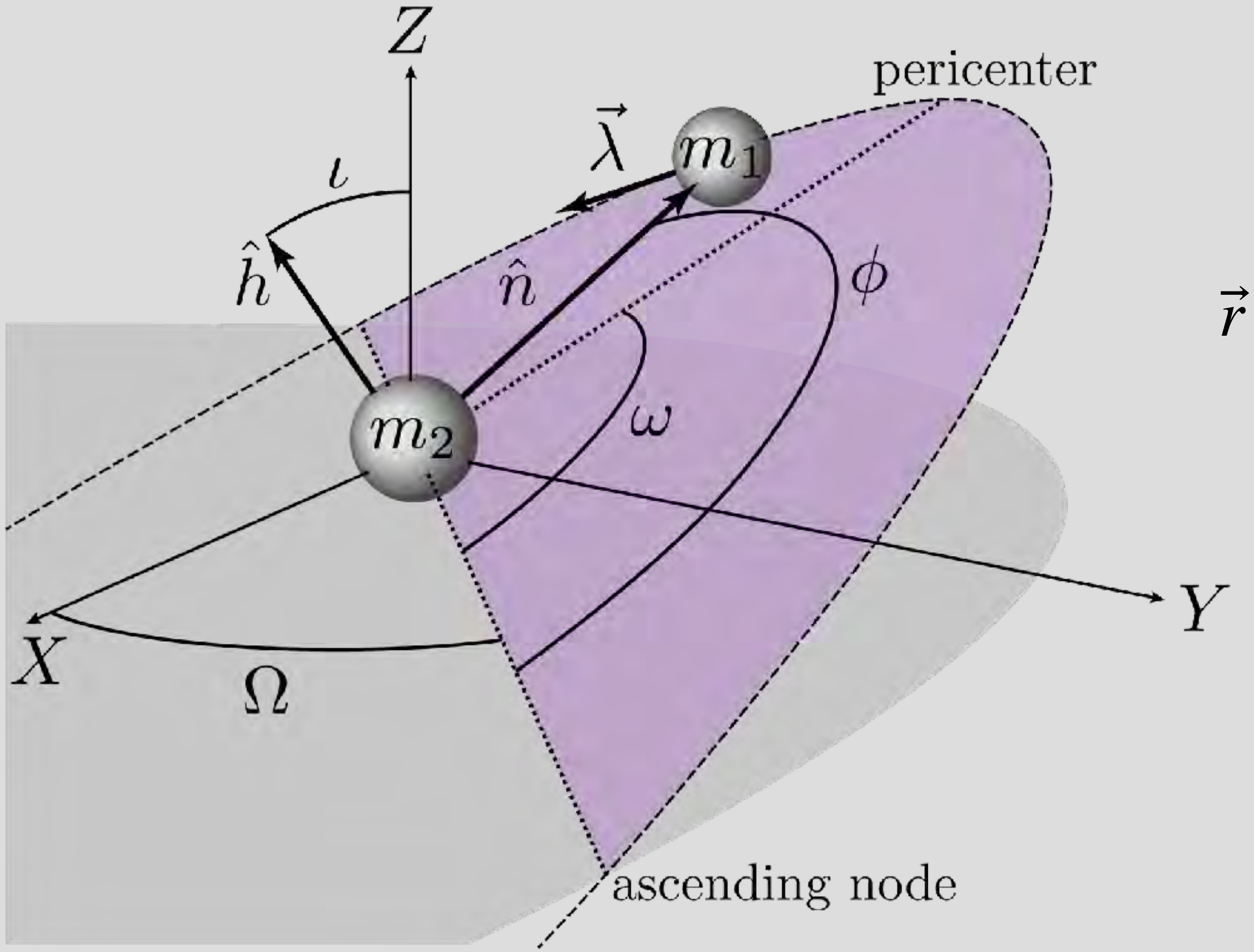

Tucker & Will, in Press, *Phys. Rev. D* arXiv:2108.12210

Schwarzschild

$$\iota \to 0 \quad \Omega \to 0 \quad \mathcal{W} \to 0$$

Effective one body problem

$$\vec{r} \equiv \vec{r}_1 - \vec{r}_2 \qquad m \equiv m_1 + m_2 \qquad \eta = \frac{m_1 m_2}{m^2}$$

Orbital Elements

$$\vec{r} \equiv \frac{p}{1 + e\cos(\phi - \omega)}\hat{n} \qquad \vec{h} \equiv \sqrt{Gmp}\,\hat{h}$$

$$p = a(1 - e^2)$$

Osculating orbit elements

$$\delta\vec{a} = \mathcal{R}\hat{n} + \mathcal{S}\hat{\lambda} + \mathcal{W}\hat{h}$$

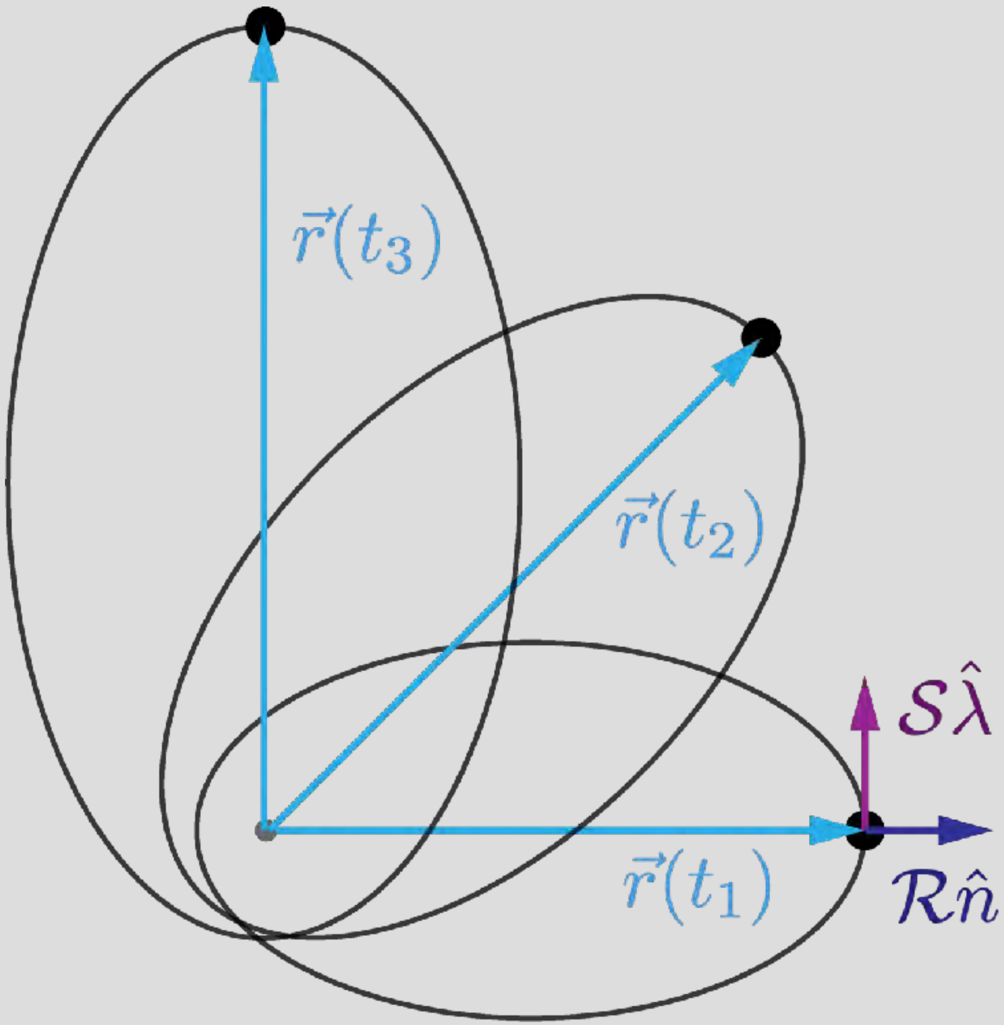

Lagrange planetary equations

$$\underbrace{\frac{dp}{d\phi} \qquad \frac{de}{d\phi}}$$

$$\frac{dX_\gamma(\phi)}{d\phi} = \epsilon Q_\gamma(X_\delta(\phi), \phi)$$

Tucker & Will, in Press, *Phys. Rev. D* arXiv:2108.12210

Scope and approach

Initial eccentricity ≈ 0.999 Arbitrary mass ratios η Schwarzschild limit (spin = 0)

post-Newtonian theory

Osculating orbit elements

Two-timescale analysis

Tucker & Will, in Press, *Phys. Rev. D* arXiv:2108.12210

Two-timescale analysis

$$\frac{dX_\gamma(\phi)}{d\phi} = \epsilon Q_\gamma(X_\delta(\phi), \phi)$$

Two-scale Ansatz

$$\theta \equiv \epsilon\phi$$

$$X_\gamma(\theta, \phi) \equiv \tilde{X}_\gamma(\theta) + \epsilon Y_\gamma\left(\tilde{X}_\delta(\theta), \phi\right)$$

Periodic

$$\langle Y_\gamma(\tilde{X}_\delta(\theta), \phi)\rangle = 0$$

$$\partial Y_\gamma / \partial\phi$$

Secular

$$\tilde{X}_\gamma(\theta) = \langle X_\gamma(\theta, \phi)\rangle$$

$$d\tilde{X}_\lambda / d\theta$$

Tucker & Will, in Press, *Phys. Rev. D* arXiv:2108.12210

Scope and approach

Initial eccentricity ≈ 0.999 Arbitrary mass ratios η Schwarzschild limit (spin = 0)

post-Newtonian theory

Osculating orbit elements

Two-timescale analysis

→**coupled secular evolution equations for p &e**

↳evolve numerically with respect to time

↳terminate when p crosses LIGO-Virgo detectable threshold

↳find analytic fit for $e(p)$

Tucker & Will, in Press, *Phys. Rev. D* arXiv:2108.12210

Evolution equations

$$x \equiv \frac{c^2 p}{Gm}$$

$$\frac{de}{d\theta} = -\frac{1}{15}\eta e x^{-5/2}(304 + 121e^2)$$
$$+\frac{1}{30}\eta e x^{-7/2}\left[\frac{1}{28}(144392 - 34768e^2 - 2251e^4) + (1272 - 1829e^2 - 538e^4)\eta\right]$$
$$-\frac{1}{34560}\eta\pi e x^{-4}(4538880 + 6876288e^2 + 581208e^4 + 623e^6)$$
$$-\frac{1}{120}\eta e x^{-9/2}\left[\frac{1}{252}(43837360 + 4258932e^2 - 1211290e^4 + 77535e^6)\right.$$
$$\left.+\frac{1}{14}(1239608 - 3232202e^2 + 898433e^4 + 13130e^6)\eta - (9216 + 24353e^2 + 45704e^4 + 4304e^6)\eta^2\right]$$

$$\frac{dx}{d\theta} = -\frac{8}{5}\eta x^{-3/2}(8 + 7e^2)$$
$$+\frac{1}{15}\eta x^{-5/2}\left[\frac{1}{14}(22072 - 6064e^2 - 1483e^4) + 4(36 - 127e^2 - 79e^4)\eta\right]$$
$$-\frac{1}{360}\eta\pi x^{-3}(18432 + 55872e^2 + 7056e^4 - 49e^6)$$
$$-\frac{1}{15}\eta x^{-7/2}\left[\frac{1}{756}(8272600 + 777972e^2 - 947991e^4 - 4743e^6)\right.$$
$$\left.+\frac{1}{84}(232328 - 1581612e^2 + 598485e^4 + 6300e^6)\eta - (384 + 1025e^2 + 5276e^4 + 632e^6)\eta^2\right]$$

Tucker & Will, in Press, *Phys. Rev. D* arXiv:2108.12210

LIGO-Virgo threshold

$$f_{GW} \approx \frac{1}{\pi}\frac{\sqrt{Gm}}{p^{3/2}}$$

$$p_f = 47.12 \left(\frac{20 M_\odot}{m} \frac{10\,\mathrm{Hz}}{f} \right)^{2/3}$$

Tucker & Will, in Press, *Phys. Rev. D* arXiv:2108.12210

Final eccentricity vs. total mass

$$x \equiv \frac{c^2 p}{Gm}$$

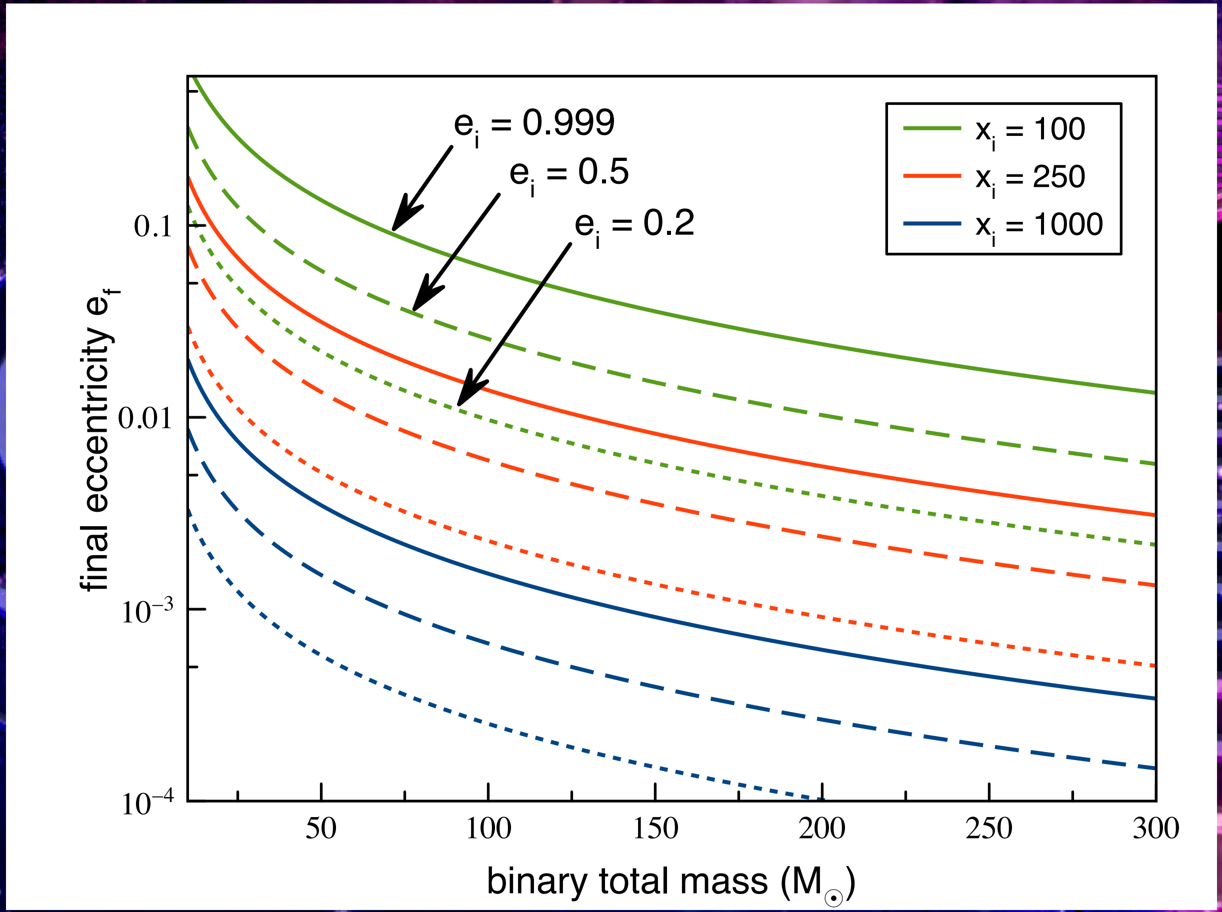

Takeaway

- ✳The **smaller** the initial values of p, the **larger** the residual e — less time to circularize
- ✳The **smaller** the mass, the **larger** the residual e — lower mass crosses 10 Hz threshold at larger p — less time to circularize

Tucker & Will, in Press, *Phys. Rev. D* arXiv:2108.12210

Mass ratio dependence

$$\eta = \frac{m_1 m_2}{m_1 + m_2}$$

- test mass limit: η → 0
- equal masses: η = ¼

$$x \equiv \frac{c^2 p}{Gm}$$

$x_f = 16 \rightarrow m = 100_\odot$ & $f = 10$ Hz

for equal-mass and test mass limit

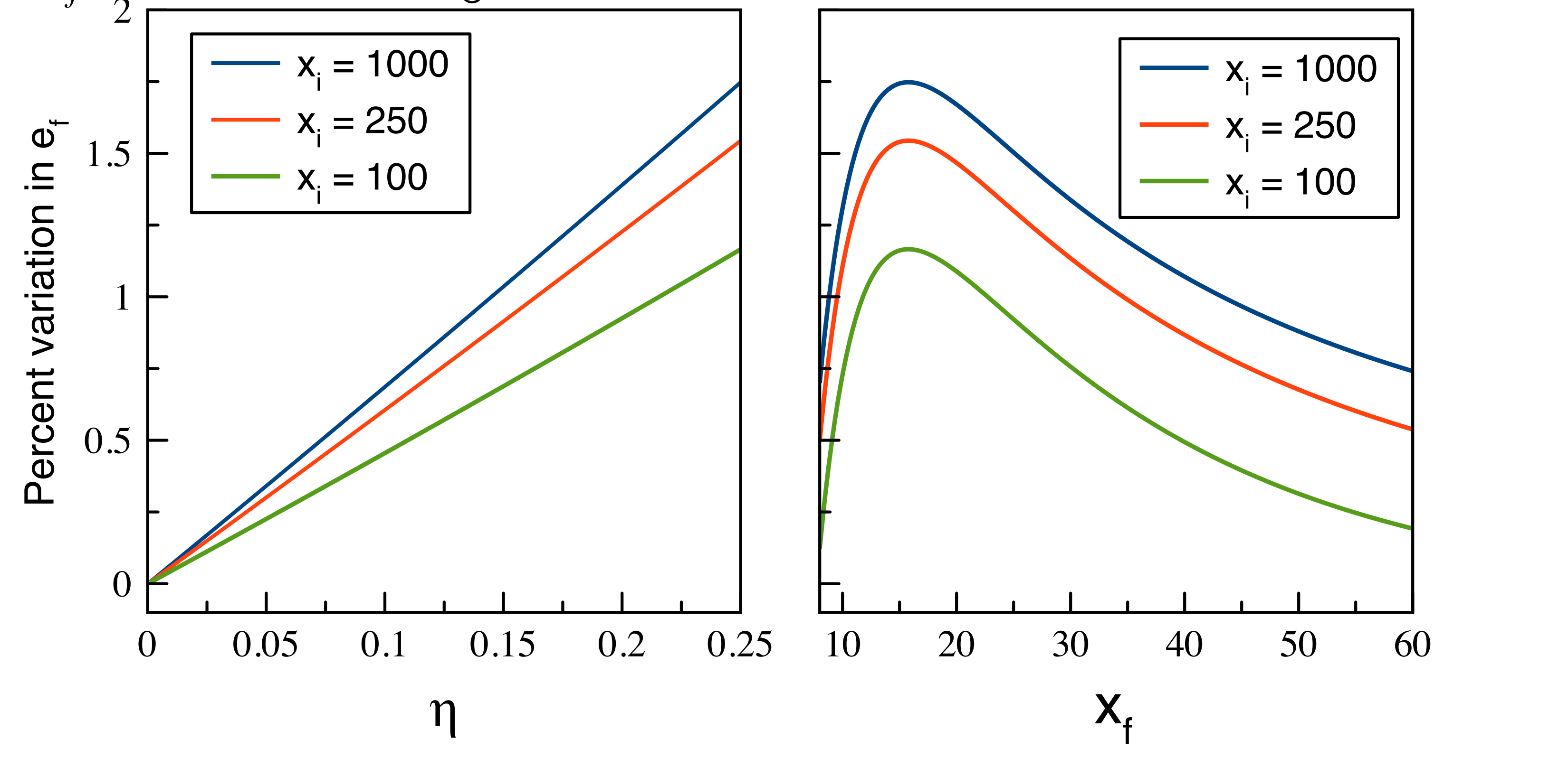

Takeaway

- ✳ e_f independent of η to better than 2 %
- ✳ Choose $\eta = 5 \times 10^{-5}$

Tucker & Will, in Press, *Phys. Rev. D* arXiv:2108.12210

5.5 PN convergence

Sago & Fujita 2015

$$\left.\frac{dx}{d\theta}\right|_{5.5} = \frac{\eta x^{-9/2}}{87318000}(294262221896 - 621776393808e^2 - 658790352267e^4 - 277665065676e^6)$$

$$\left.\frac{de}{d\theta}\right|_{5.5} = \frac{\eta e x^{-11/2}}{349272000}(1790315545528 - 6186148025656e^2 - 4964186588931e^4)$$

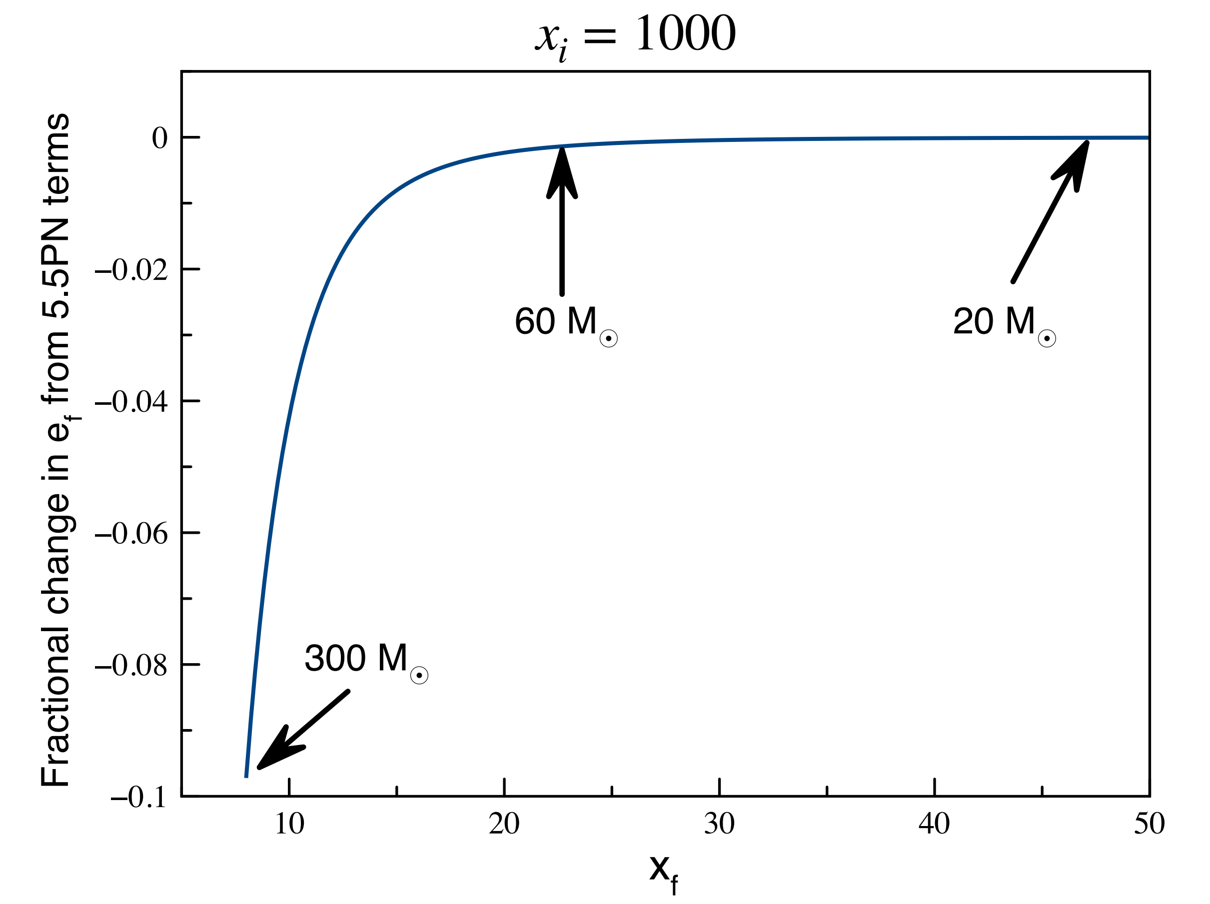

Takeaway

Small effect except for the most massive systems which are very relativistic when they cross the threshold

Tucker & Will, in Press, *Phys. Rev. D* arXiv:2108.12210

Eccentricity map

Lowest order textbook solution (Peters & Mathews 1963)

$$x = x_i \frac{g(e)}{g(e_i)} \quad \text{with} \quad g(e) = e^{12/19}\left(304 + 121e^2\right)^{870/2299}$$

PN-corrected

$$x = x_i \left(\frac{1+2/x_i}{1+2/x}\right)\left(\frac{1-4/x_i}{1-4/x}\right)^{12/19} \frac{g(e)}{g(e_i)}$$

$$e = g^{-1}\left[\frac{x}{x_i}\left(\frac{1+2/x}{1+2/x_i}\right)\left(\frac{1-4/x}{1-4/x_i}\right)^{12/19} g(e_i)\right]$$

Analytic fits

$$x \equiv \frac{c^2 p}{Gm}$$

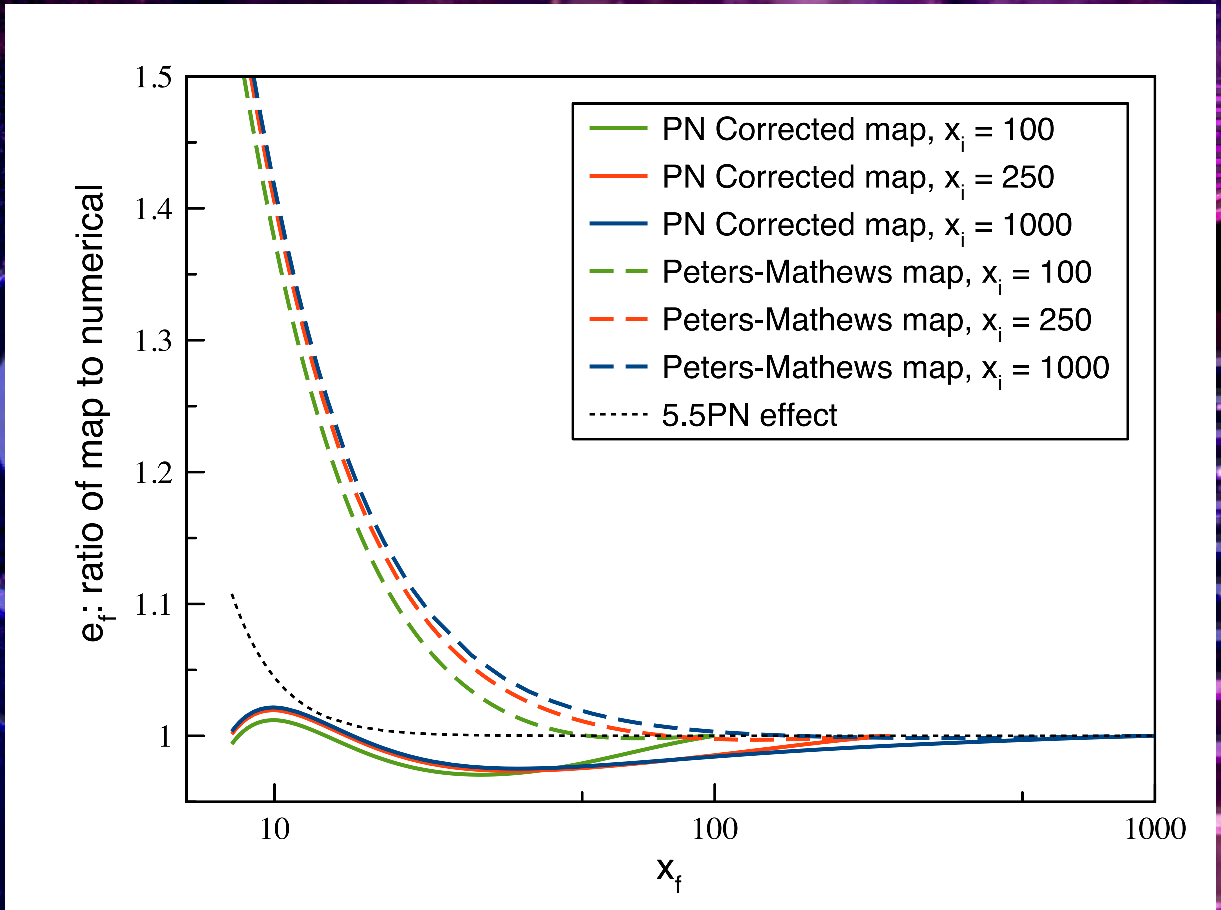

Takeaway

- ✳PN-corrected map better than $2\,\%$ agreement with numerical solutions
- ✳PN-corrected values systematically smaller than Peters-Mathews by as much as $30\,\%$ for $60\,\mathrm{M}_\odot$ crossing LIGO-Virgo threshold at 10 Hz.

Tucker & Will, in Press, *Phys. Rev. D* arXiv:2108.12210

Accuracy of PN

$$x \equiv \frac{c^2 p}{Gm}$$

PN corrections on values of e_f compared to Peters-Mathews

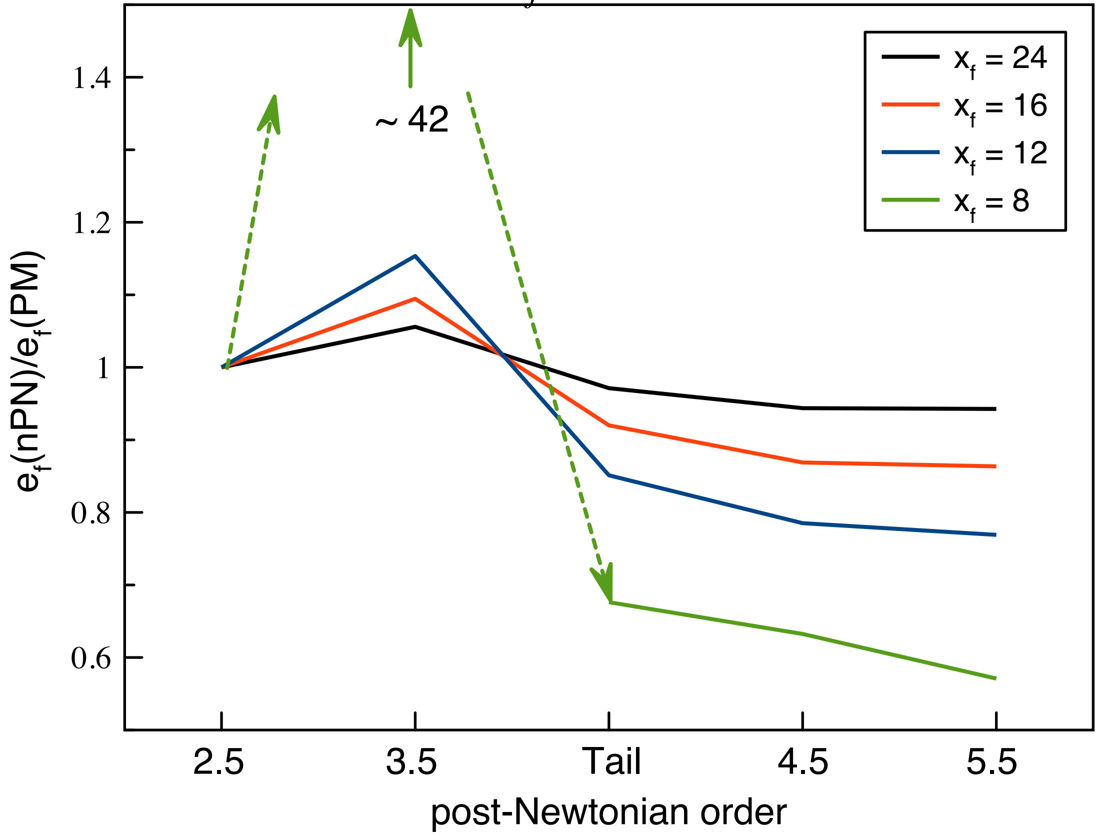

Takeaway

- ✳2.5PN order numerical results agree with PM values
- ✳3.5PN order has a sign difference, causing e to grow, especially at highly relativistic distances
- ✳adding additional PN terms mitigates this behavior

Tucker & Will, in Press, *Phys. Rev. D* arXiv:2108.12210

Conclusion

Summary

- ✳Used PN equations of motion including RR to 4.5PN to analyse late-time eccentricities of non-spinning binaries of arbitrary masses
- ✳Found that final eccentrics are essentially independent of η
- ✳Found a PN-corrected analytic map for final eccentricities that produces consistently smaller values than lowest order map by as much as $60\,\%$ and agrees with numerically generated values to a few percent

Potential application

- ✳Assessing the levels of orbital eccentricity that must be incorporated into GW templates
- ✳Relating measured late-time eccentricities to astrophysical origins of compact binary inspirals

Future work

- ✳Extend work to **include spin-orbit**
- ✳Derive a **probability distribution** of final eccentricity as a function of the initial astrophysical environment

Tucker & Will, in Press, *Phys. Rev. D* arXiv:2108.12210